Materials Science and Engineering B 297 (2023) 116726

Contents lists available at ScienceDirect

Materials Science & Engineering B

journal homepage: www.elsevier.com/locate/mseb

Fabrication of Epoxy-CuInS-ZnS QDs- nanocomposite for fluorescent, transparent toughened coating applications

Vasudevan Pillay R. Remya [a,b], Sundararajan Parani [a,b,d], Jose V. Rajendran [b], Rodney Maluleke [a,b], Thabang C. Lebepe [a,b], Olanrewaju A. Aladesuyi [a,b], Sabu Thomas [a,b,c,*], Oluwatobi S. Oluwafemi [a,b,*]

[a] Department of Chemical Sciences (formerly Applied Chemistry), University of Johannesburg, P.O. Box 17011, Doornfontein 2028, Johannesburg, South Africa
[b] Centre for Nanomaterials Science Research, University of Johannesburg, Johannesburg, South Africa
[c] International and Inter-University Centre for Nanoscience and Nanotechnology, School of Energy Materials, Mahatma Gandhi University, Kottayam, India
[d] Department of Electrical and Computer Engineering, Sungkyunkwan University, Jangan-Gu, Suwon, Gyeonggi-do 16419, South Korea

ARTICLE INFO

Keywords:
Copper Indium sulfide
Quantum dots
Epoxy nanocomposites
Luminescent
Toughened

ABSTRACT

We herein report a simple method for preparing luminescent and highly toughened transparent epoxy/copper indium sulfide-zinc sulfide (CIS-ZnS) nanocomposite for coating applications. Briefly, fluorescent organically soluble dodecanethiol-capped CIS-ZnS core–shell quantum dots (QDs) was prepared via a solvothermal method. The as-synthesized QDs were small, spherical and highly crystalline, with an average particle diameter of 2.7 nm and improved photoluminescence quantum yields. The QDs were then dispersed in an epoxy matrix to produce a luminescent, transparent, and toughened nanocomposite with excellent mechanical properties: 5348.45 ± 58 J/m^2 impact strength value (90 % better than epoxy system only), 34.6 ± 2.8 MPa tensile strength and 6.55 ± 0.31% elongation at break value (significant increment compared to the neat epoxy system). The proposed method is facile and efficient in preparing luminescent, transparent and toughened surface coating materials, which could be used for various physical and automobile applications.

1. Introduction

Over the past two decades, semiconductor nanoparticles known as quantum dots (QDs) have shown great promise in light emitters, fluorescent coatings and biological imaging applications [1–9]. While much interest has been obtained using binary II-VI QDs, they are mostly characterized with heavy metal toxicity (Cd, Hg) which are potentially harmful to humans and the environment [10,11]. Consequently, other materials have been regarded as substitutes, such as binary III-V compounds and ternary I-III-VI compounds. Due to their high coefficient of absorption and non-toxic makeup, I-III-VI chalcopyrite QDs like $CuInSe_2$ (CISe), $AgInS_2$ (AIS), $CuInS_2$ (CIS), and $AgGaS_2$ (AGS) have received the most attention [6,12–23].

Most researchers have recently shifted their focus from synthesis to applications of these QDs materials [24–28]. Due to their physical characteristics, such as light weight and endurance when compared to other matrices like metals and ceramics, polymers are one of the most popular and, along with QDs, the best options for high-end applications [29–31]. In this regard, epoxy resin has shown to be the optimal polymer matrix candidate due to its high glass transition temperature, superior transparency, and low water absorption during end-product manufacturing [29,30,32–35]. QDs have become one of the most important and efficient epoxy modifiers among nanomaterials due to their significant potential for use in electronics, photonics, optoelectronics, structural, and bio-applications. One of the crucial elements affecting the epoxy nanocomposite's optical characteristics is the effective dispersion of the QDs inside the polymer matrices [33,36–41].

Wang and Sun *et al.* synthesized CdSe/CdS/ZnS core/multi-shell QDs for the first time in paraffin liquid via a phosphine-free process [42]. Transparent and fluorescent epoxy/ CdSe-CdS-ZnS core-multi shell QD polymer nanocomposites with superior mechanical properties compared to the neat polymer matrix have been successfully reported by Sneha and colleagues [33]-However, as far as the authors know, no work has been published on the synthesis and application of epoxy-ternary QDs

* Corresponding authors at: Department of Chemical Sciences (formerly Applied Chemistry), University of Johannesburg, P.O. Box 17011, Doornfontein 2028, Johannesburg, South Africa.
E-mail addresses: sabuthomas@mgu.ac.in (S. Thomas), oluwafemi.oluwatobi@gmail.com (O.S. Oluwafemi).

https://doi.org/10.1016/j.mseb.2023.116726
Received 2 February 2023; Received in revised form 11 June 2023; Accepted 9 July 2023
Available online 22 July 2023

composites. In this paper, we describe the fabrication of toughened epoxy/CIS-ZnS core–shell QDs nanocomposites that are extremely luminous. The as-synthesized nanocomposite exhibited dual properties, i.e. fluorescent and mechanical properties. The reported method is novel, facile and useful for fluorescent and toughened coating applications.

2. Experimental methods

2.1. Materials

Copper Iodide (CuI), indium acetate ($InAc_3$), zinc acetate, 1-octadecene, 1-dodecanethiol (>98%), chloroform, hexane and acetone were purchased from Sigma Aldrich, South Africa. Atul Ltd. in India provided the Lapox L12, diglycidyl ether of bisphenol-A (DGEBA), epoxy resin (mean epoxy equivalent weight 182–192 gm/eq), and Lapox-K5, 4, 4′-diaminodiphenylmethane (DDM).

2.2. Sample preparation

2.2.1. Synthesis of dodecanethiol (DDT) capped CIS-ZnS core–shell QDs

In a typical synthesis, CuI (0.25 mmol, 0.0476 g) and $In(Ac)_3$ (1.0 mmol, 0.2920 g) were added to a Teflon-lined autoclave. 20 mL of 1 dodecanethiol (DDT), which serves as both a solvent and a sulfur precursor, was then added to the above mixture. The autoclave was then heated to a temperature of 180 °C for 5 h followed by cooling at room temperature. A reddish solution was seen in the autoclave container, indicating the formation of core CIS QDs. A consecutive ZnS shell overcoating was performed over core CIS QDs by adding Zn acetate (8 mmol, 1.7650 g), DDT (2 mL), and 1-octadecence (ODE) (8 mL) to the crude CIS solution and heated to 200 °C for 14 h in the autoclave. After cooling to room temperature, a yellowish-orange core–shell CIS- ZnS QDs was obtained, which was then dispersed in chloroform. The QDs was then isolated from the solution by precipitation with acetone, followed by centrifugation and drying. Scheme 1 shows a schematic representation of the preparation of DDT capped core CIS and CIS-ZnS core–shell QDs.

2.2.2. Preparation of epoxy/ (DDT) capped CIS-ZnS core–shell QDs nanocomposite:

The epoxy/QDs nanocomposites were prepared by the melt mixing technique. Typically, core-multi-shell QDs solution (0.2 wt%) was mixed with epoxy resin by probe-sonication at room temperature for 15 mins followed by magnetic stirring at 80 °C. The stoichiometric volume of DDM (4.4 ’diamino diphenyl methane) hardener was then applied to the system after full elimination of bubbles and stirred at 90 °C for 10 mins. It was then poured into the pre-heated mould and cured for 3 h at 90 °C and then post-cured for 3 h at 170 °C. The samples were then allowed to cool to ambient temperature and cut to the necessary dimensions for characterization. The same reaction conditions were used to cure neat epoxy resin for comparison.

2.3. Characterization techniques:

The PL. emission spectra were collected using a spectrophotometer made by Shimadzu, Japan (RF-6000). The following equation was used to determine the photoluminescence quantum yield (PLQY),

$$\phi_s = \left(\frac{I_S}{I_R}\right) * \left(\frac{A_R}{A_S}\right) * \left(\frac{n_s^2}{n_R^2}\right) * \phi_{R*100}$$

where Φ_S and Φ_R are the sample and reference quantum yield, I_S and I_R are the sample and reference integrated intensities, A_S and A_R are the sample and reference excitation wavelength absorbance, and n_S and n_R are the sample and reference refractive indices, respectively. The reference standard was a rhodamine 6G ethanol solution with a quantum yield of $\Phi_R = 0.95$. Measurements of absorption spectra were carried out in the wavelength range between 200 and 900 nm using the Perkin Elmer Lambda 25 UV–Vis spectrophotometer. Fourier transform infrared spectroscopy (FTIR) analysis was carried out using Spectrum two Universal Attenuated Total Reflection (UATR) spectrometers. Transmission electron microscope (TEM) images and selected area electron diffraction (SAED) patterns of CIS and CIS-ZnS QDs were obtained with a JEOL JEM − 2100 microscope. The chemical composition of CIS and CIS-ZnS QDs was determined by energy-dispersive spectroscopy (EDS) attached to the TEM. The XRD patterns were obtained on a Bruker D8 Advance diffractometer using monochromatic Cu-Kα1 radiation (λ = 1.5406 Å). The tensile tests of the neat epoxy and epoxy/QDs nanocomposites were conducted at room temperature with a Tinius Olsen H50KT testing machine for Type I measurement according to ASTM D638. For notched specimens with dimensions of 63.5x 12.7x 3 mm, the Izod impact strength of the neat epoxy and epoxy/QDs nanocomposites was analyzed at room temperature as indicated in ASTM D256 using a Zwick Roel HIT25P impact tester machine with 5.5 J at 23 °C as per ASTM D 256.

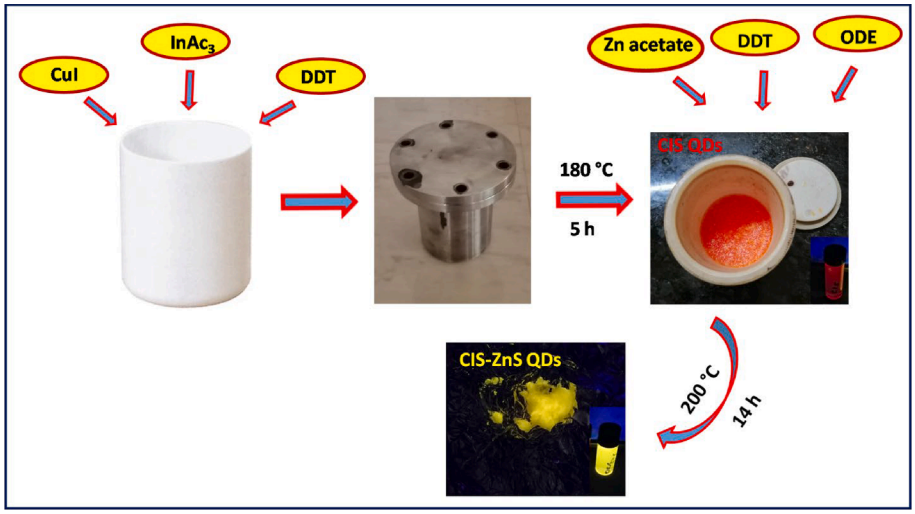

Scheme 1. Synthesis of DDT capped CIS core QDs and CIS-ZnS core–shell QDs.

3. Results and discussions

3.1. Optical properties of DDT capped CIS core and CIS-ZnS core–shell QDs:

The synthesis of QDs was carried out in the organic phase by using solvothermal method. For CIS core QDs synthesis, the Cu:In ratio was maintained at 1:4 as this ratio has been reported in the literature to produce the CIS QDs with excellent optical properties [2,14,43–46]. The ZnS shell was then grown over the CIS QDs to improve its optical properties further. The absorption spectra of CIS core and CIS-ZnS core–shell QDs are shown in Fig. 1a; CIS QDs exhibit a broad absorption peak at 481 nm, whereas the CIS-ZnS core–shell QDs exhibit an absorption peak at 472 nm. The corresponding PL spectra were shown in Fig. 1b where CIS core QDs exhibit a broad peak centred at 626 nm while CIS-ZnS QDs were observed at 586 nm. The observed blue shift of CIS-ZnS QDs in both the absorption and PL spectra, when compared to core CIS QDs, is attributed to the partial diffusion of Zn ions from the shell to the core, which enlarges the bandgap of the core CIS QDs. The growth of ZnS increased the PL intensity of the QDs, indicating the passivation of the core QDs defect sites. This blue-shift emission and the enhanced fluorescence were also observed visually in the fluorescent images under UV lamp where CIS core QDs displayed red emission with weak intensity while CIS-ZnS core–shell QDs showed bright and yellow emission (Fig. 1d). Consequently, the PLQY of CIS QDs and CIS-ZnS core–shell QDs were measured to be 3.5 and 24.3 %, respectively.

3.2. FTIR Studies:

The surface chemistry of the as-produced QDs was investigated using the FTIR (Fig. 2). The FTIR spectrum of DDT revealed three distinct absorption peaks around 2950 cm^{-1}, 2923 $cm^{-1,}$ and 2853 cm^{-1}, attributed to the asymmetric stretching of CH_3, the asymmetric stretching of CH_2 and the symmetric stretching of CH_2, respectively. The other distinct peaks in DDT around 1500 cm^{-1} and 700 cm^{-1} are attributed to CH_2 wagging and C-S stretching vibrations, respectively. These peaks were also present in the QDs, suggesting that QDs were capped by DDT. Therefore, it can be clearly proved that the surface ligand is DDT.

3.3. TEM and EDS studies:

The TEM micrographs of the as-synthesized QDs (Fig. 3 a and b) show that they are small and spherical. The particle size of CIS QDs (Fg. 3e) was within the range of 1.8 nm to 3.0 nm, with an average particle diameter of 2.1 nm, while that of CIS-ZnS core–shell QDs (Fig. 3f) was found to be in the range of 2.2 nm to 3.2 nm with an average particle diameter of 2.7 nm. The broad size distribution is due to the synthesis based on non-injection and can be partly attributed to the continuous release of S^{2-} from the DDT molecule during the reaction [4].The

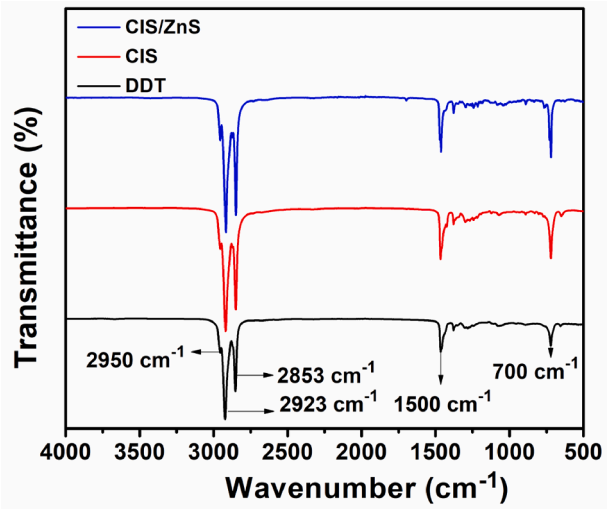

Fig.2. FTIR spectra of DDT, CIS and CIS-ZnS QDs.

increased particle size of CIS-ZnS QDs showed the deposition of ZnS shell over core CIS QDs. The HRTEM micrographs of the as-prepared QDs also showed distinct lattice fringes [Fig. 3 (a) and (b)] inset] demonstrating the crystallinity of the QDs. The presence of the elements Cu, In, S for CIS QDs and Cu, In, Zn and S for CIS-ZnS QDs were confirmed by the EDS (Fig. 3c and d).

3.4. Crystal structure of CIS and CIS-ZnS QDs [XRD and SAED]:

The SAED and XRD patterns of CIS QDs and CIS-ZnS core–shell QDs are shown in Fig. 4. For CIS QDs, three significant diffraction peaks with 2θ values of 28°, 46.5°, and 54.9° are observed. These peaks are well indexed to the (1 1 2), (2 0 4), and (3 1 2) planes of the known $CuInS_2$ phase tetragonal chalcopyrite (JCPDS 85–1575) structure [15]. The XRD peak positions changed to a higher 2θ value after the ZnS shell formation. The observed broadness of XRD peaks could be attributed to the nanocrystalline nature of the QDs, which is also confirmed by ring patterns in the selected area electron diffraction (SAED).

3.5. Optical properties of epoxy/ CIS-ZnS QDs nanocomposite:

The PL spectra of epoxy/CIS-ZnS QDs nanocomposites (0.2 wt%) excited at 380 nm are shown in Fig. 5. The maximum emission wavelength of the neat epoxy (cured) was observed at 454 nm, which increased to 491 nm in the core–shell nanocomposite. In addition, the PL intensity of the epoxy increased after the dispersion of the fluorescent QDs. This is further supported by the photographic image obtained under the UV lamp (365 nm). The neat epoxy showed blue emission [Fig. 5(b)] while the epoxy/ CIS-ZnS QDs (0.2 wt%) nanocomposite

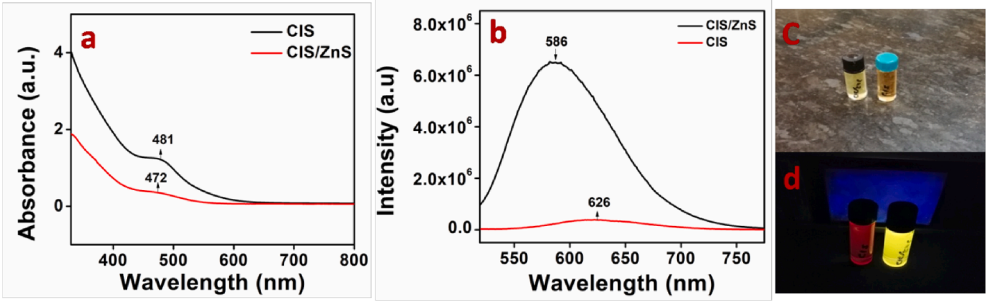

Fig.1. (a) UV–Visible spectra of CIS and CIS-ZnS QDs; (b) Photoluminescence (PL λ_{exc} = 450 nm) spectra of CIS and CIS-ZnS QDs, (c) & (d) shows the photographic images of CIS and CIS-ZnS QDs under room light and UV lamp (red-CIS and Yellow-CIS-ZnS), respectively. (For interpretation of the references to colour in this figure legend, the reader is referred to the web version of this article.)

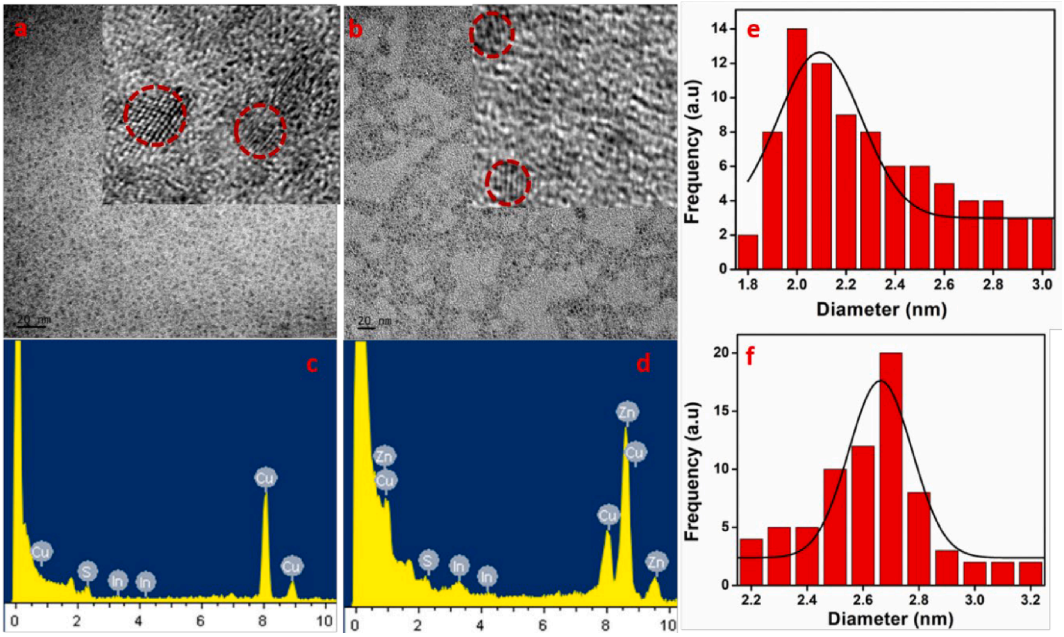

Fig.3. TEM images of (a) CIS QDs, (b) CIS-ZnS QDs, (Insets: HRTEM images showing crystallinity of the QDs. EDS patterns of (c) CIS QDs, (d) CIS-ZnS QDs, (e) and (f) are the corresponding particle size distribution.

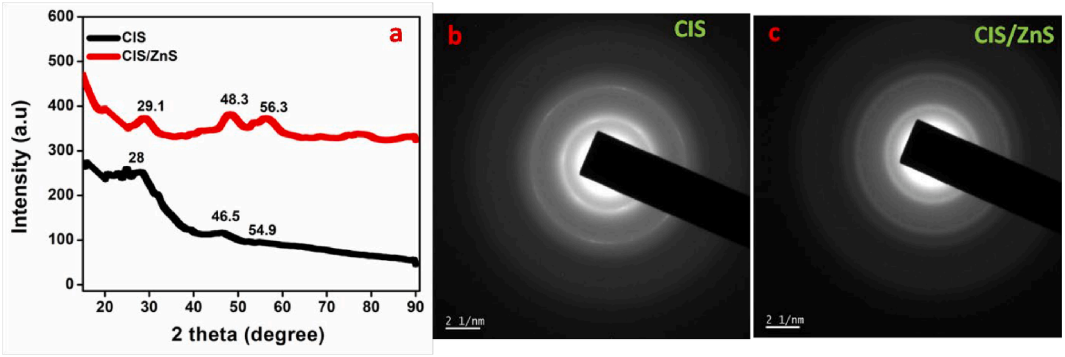

Fig.4. (a) XRD patterns, (b) and (c) are SAED patterns of CIS and CIS-ZnS QDs.

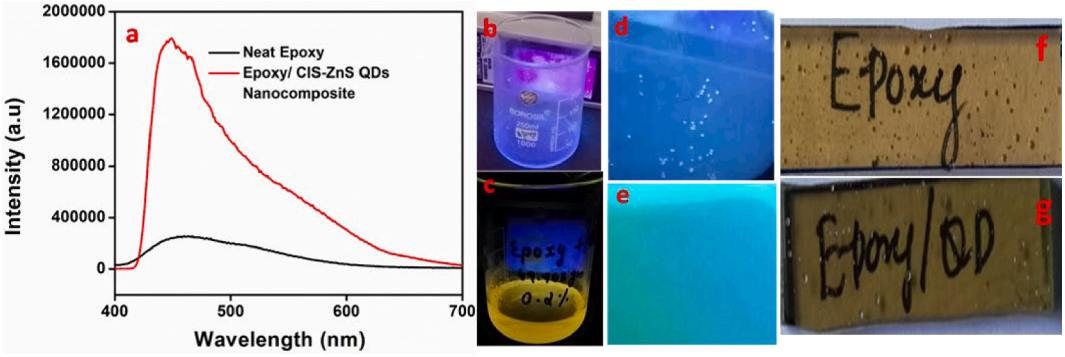

Fig.5. (a) PL spectra of neat epoxy and epoxy/CIS-ZnS core–shell QDs nanocomposite; (b) & (c) are the photographs of neat epoxy and epoxy/CIS-ZnS core–shell QDs nanocomposite before curing and (d) & (e) after curing under the UV lamp (365 nm), respectively. The transparency of the neat epoxy (f) and epoxy-QDs (g) after curing.

showed bright yellow emission [Fig. 5(c)] like that of core–shell QDs before curing. After curing, the epoxy showed blue emission [Fig. 5(d)] while the corresponding epoxy- CIS-ZnS QDs nanocomposite showed cyan colour emission [Fig. 5 (e)]. The transparency of the neat epoxy was retained in the core–shell QDs nanocomposite [Fig. 5.(f &g)]. This is attributable to the QDs' excellent dispersion within the continuous epoxy matrix as well as the matched refractive indices of the epoxy polymer and QDs [33].

The transmission spectra of the neat epoxy and epoxy CIS-ZnS QDs nanocomposite is shown in Fig. 6. Following the addition of CIS-ZnS

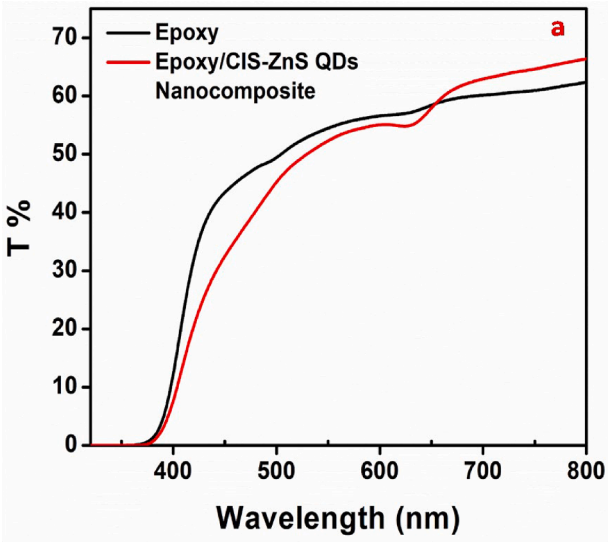

Fig.6. UV–vis transmittance of pure epoxy and epoxy/CIS-ZnS core–shell QDs nanocomposite.

QDs, it was observed that the epoxy's cut-off wavelength increased from 360 nm to 380 nm, indicating that the addition of CIS-ZnS allows the epoxy material to have greater UV resistance. The UV resistance of the as-synthesized material is very important for various applications like producing durable WLEDs, displays, luminescence coatings etc [43].

3.6. *Mechanical properties of epoxy/ CIS-ZnS QDs nanocomposite:*

3.6.1. *Tensile properties*

The tensile behaviour of the epoxy/CIS-ZnS core–shell QDs nanocomposite was analyzed, and the respective stress vs strain plots are shown in Fig. 7. Table 1 shows the appropriate Young's modulus, tensile strength, and elongation at break values.

It is seen from the tensile strength results that the addition of core–shell QDs significantly improved the tensile properties of the epoxy nanocomposite. The tensile modulus, tensile strength and elongation at break of the epoxy thermoset were substantially improved after the addition of CIS-ZnS QDs. The region under the stress–strain curve Fig. 7 (a) reflects the energy absorbed during stretching and shows the material's toughness. Table 1 showed that after the dispersion of CIS-ZnS QDs, the strength and elongation at the break of epoxy were enhanced. This indicates that CIS-ZnS core–shell QDs play an important role in the production of a highly toughened fluorescent material in the epoxy matrix. The strong increase in epoxy nanocomposite tensile parameters is attributed to the CIS-ZnS particle reinforcement and increased dispersion as the QDs act as epoxy thermoset filler. The DDT

Table 1
Tensile parameters of neat epoxy and epoxy/Q.D.s nanocomposite.

Sample	Tensile modulus (MPa)	Tensile strength (MPa)	Elongation at break (%)	Toughness (J/m^3)
Neat Epoxy	1420 ± 72	29.4 ± 3.2	5.43 ± 0.37	84. 28
Epoxy/CIS-ZnS core–shell QDs nanocomposites	1600 ± 63	34.6 ± 2.8	6.55 ± 0.31	102.14

capping makes the surface hydrophobic on the surface of CIS-ZnS core–shell QDs and helps to mix with the epoxy easily. In addition, the QDs filled the voids already present in the epoxy matrix, resulting in a decrease in free volume (Scheme 2). These factors combined give epoxy/QDs nanocomposites strong tensile properties and stiffening effects.

3.6.2. *Impact Strength:*

The pendulum impact test results of the neat epoxy and epoxy/CIS-ZnS QDs composites are shown in Fig. 7 (b) and Table 2. The impact test results clearly demonstrated the toughness of the material produced. The results showed that the impact strength of the epoxy was substantially improved by 90 % after the addition of CIS-ZnS core–shell QDs. The system's impact energy was also associated with impact strength and showed enhancement in the composite which is suitable for the extremely toughened framework.

It is known that a neat epoxy system works like a glassy material. Under the application of load, a uniform and normal orientation of cracks will appear, which would then quickly propagate and then break the substance. In the case of nanocomposite like this epoxy/ CIS-ZnS QDs, the crack is deflected in various directions, pinned with each spherical QDs and propagated during the load application through these domains. By means of the familiar crack top, this process takes a longer path and dissipates more energy. In addition, each QD in the cross-linked epoxy matrix serves as a filler and promotes outstanding toughness.

4. Conclusions

In this study, red-emitting DDT capped CIS core QDs, and yellow-emitting CIS-ZnS core–shell QDs were successfully synthesized by using solvothermal method. The TEM and XRD analyses showed that the QDs were small, highly crystalline, and well dispersed. FTIR results confirmed the DDT capping on the QDs. After the formation of ZnS shell, the maximum emission peak shifted to a shorter wavelength (626 nm → 586 nm), and the PLQY increased significantly from 3.45 % (core) to 24.34 % (core–shell). The DDT capped CIS-ZnS core–shell QDs were then integrated into an epoxy resin. The incorporation of yellow emitting CIS-ZnS-core–shell QDs in the epoxy polymer shifted the emission of the epoxy from blue to cyan. The addition of CIS-ZnS core–shell QDs

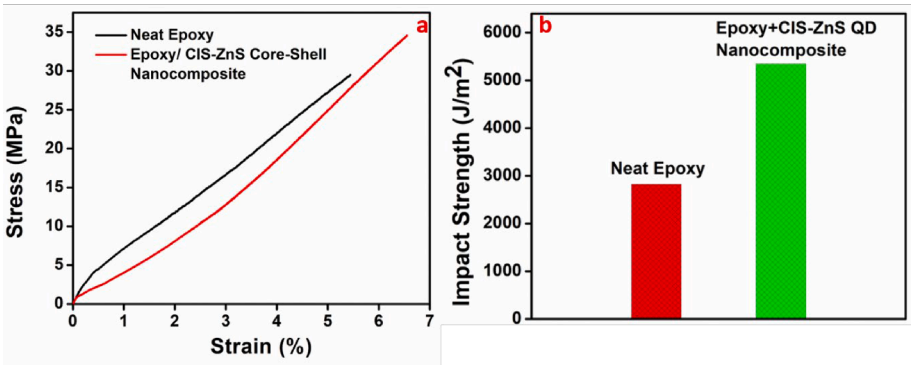

Fig.7. (a) The stress–strain curve and (b) impact strength of pure epoxy and epoxy-CIS-ZnS QDs nanocomposite.

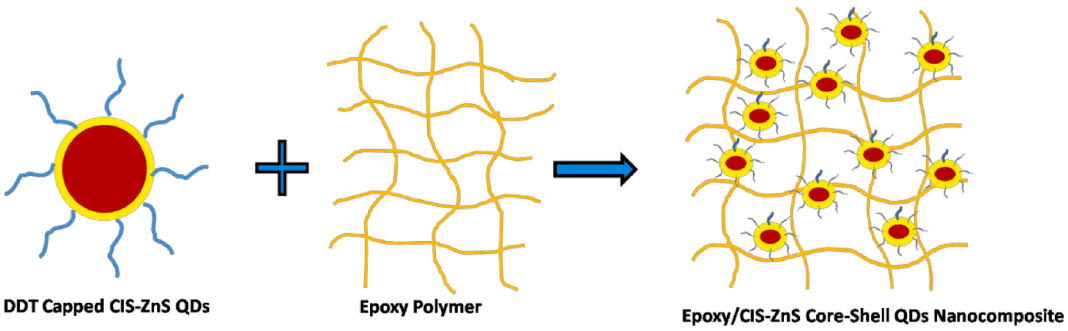

Scheme 2. Schematic representation of the interaction of the DDT capped CIS-ZnS core–shell QDs with epoxy resin.

Table 2
Impact properties of neat epoxy and epoxy/Q.D.s nanocomposite.

Sample	Impact Strength (J/m^2)	Impact Energy (J/m)
Neat epoxy	2824. 43 ± 44.20	30.22 ± 3.24
Epoxy/CIS-ZnS core–shell QDs nanocomposites	5348. 45 ± 58.24	56.87 ± 6.20

significantly increases the UV resistance of the neat epoxy. The epoxy/CIS-ZnS QDs' tensile strength improved significantly after the dispersion of the QDs in the epoxy matrix, while the impact strength tests revealed improved toughness. In conclusion, a luminescent, transparent, and toughened epoxy/CIS-ZnS core–shell nanocomposite has been developed, which can be used for a variety of applications such as fluorescent-toughened surface coatings, flooring, aircrafts, automobiles, LEDs, and other electronic devices.

CRediT authorship contribution statement

Vasudevan Pillay R. Remya: Conceptualization, Methodology, Validation, Investigation, Writing – original draft, Visualization. **Sundararajan Parani:** Formal analysis, Writing – review & editing. **Jose V. Rajendran:** Formal analysis. **Rodney Maluleke:** Formal analysis. **Thabang C. Lebepe:** Formal analysis. **Olanrewaju A. Aladesuyi:** . **Sabu Thomas:** Conceptualization, Methodology, Validation, Resources, Writing – review & editing, Resources, Supervision, Project administration, Funding acquisition. **Oluwatobi S. Oluwafemi:** Conceptualization, Methodology, Validation, Resources, Project administration, Writing – review & editing, Supervision, Funding acquisition.

Declaration of Competing Interest

The authors declare that they have no known competing financial interests or personal relationships that could have appeared to influence the work reported in this paper.

Data availability

Data will be made available on request.

Acknowledgements

The authors acknowledge financial support from NRF South Africa under CPRR grants no. 106060 and 129290, the Faculty of Science at the University of Johannesburg in South Africa, and the Defence Research and Development Organization (DRDO), Delhi, India. We also acknowledge DST's Nanomission and PURSE Scheme for their kind support. Thanks to the the Centre for Nanomaterials Science Research at the University of Johannesburg in South Africa and International and Inter-University Centre for Nanoscience and Nanotechnology at Mahatma Gandhi University in Kerala, India, for providing necessary facilities.

References

[1] D.V. Talapin, J.-S. Lee, M.V. Kovalenko, E.V. Shevchenko, Prospects of Colloidal Nanocrystals for Electronic and Optoelectronic Applications, Chem. Rev. 110 (2009) 389–458, https://doi.org/10.1021/cr900137k.
[2] S. Hyun Park, A. Hong, J.-H. Kim, H. Yang, K. Lee, H. Seong Jang, Highly Bright Yellow-Green-Emitting CuInS2 Colloidal Quantum Dots with Core/Shell/Shell Architecture for White Light-Emitting Diodes, ACS Appl. Mater. & Interfaces. 7 (2015) 6764–6771, https://doi.org/10.1021/acsami.5b00166.
[3] A.M. Smith, H. Duan, A.M. Mohs, S. Nie, Bioconjugated quantum dots for in vivo molecular and cellular imaging, Adv. Drug Deliv. Rev. 60 (2008) 1226–1240, https://doi.org/10.1016/J.ADDR.2008.03.015.
[4] A. Aboulaich, M. Michalska, R. Schneider, A. Potdevin, J. Deschamps, R. Deloncle, G. Chadeyron, R. Mahiou, Ce-Doped YAG Nanophosphor and Red Emitting CuInS2/ZnS Core/Shell Quantum Dots for Warm White Light-Emitting Diode with High Color Rendering Index, ACS Appl. Mater. & Interfaces. 6 (2013) 252–258, https://doi.org/10.1021/am404108n.
[5] P.V. Kamat, Quantum Dot Solar Cells. Semiconductor Nanocrystals as Light Harvesters, J. Phys. Chem. C. 112 (2008) 18737–18753, https://doi.org/10.1021/jp806791s.
[6] O.S. Oluwafemi, B.M.M. May, S. Parani, N. Tsolekile, Facile, large scale synthesis of water soluble AgInSe2/ZnSe quantum dots and its cell viability assessment on different cell lines, Mater. Sci. Eng. C. 106 (2020), 110181, https://doi.org/10.1016/J.MSEC.2019.110181.
[7] S. Lee, S. Kim, J. Gim, M.H. Alfaruqi, S. Kim, V. Mathew, B. Sambandam, J. Y. Hwang, J. Kim, Ultra-small ZnS quantum dots embedded in N-doped carbon matrix for high-performance Li-ion battery anode, Compos. Part B Eng. 231 (2022), 109548, https://doi.org/10.1016/J.COMPOSITESB.2021.109548.
[8] L. He, S. Mei, Q. Chen, W. Zhang, J. Zhang, J. Zhu, G. Chen, R. Guo, Two-step synthesis of highly emissive C/ZnO hybridized quantum dots with a broad visible photoluminescence, Appl. Surf. Sci. 364 (2016) 710–717, https://doi.org/10.1016/J.APSUSC.2015.12.213.
[9] H. Zhu, Z. Liu, Z.L. Cheng, Stable dispersed N-doped carbon quantum dots-decorated 2D Ni-BDC nanocomposites towards the tribological application, Appl. Surf. Sci. 582 (2022), 152428, https://doi.org/10.1016/J.APSUSC.2022.152428.
[10] C. Zhou, X. Yang, C. Zhang, S. Zhang, P. Zhang, Fluorescent CdSe/ZnS quantum dots incorporated poly (styrene-co-maleic anhydride) nanospheres for high-sensitive C-reaction protein detection, Surfaces and Interfaces. 24 (2021), 101057, https://doi.org/10.1016/J.SURFIN.2021.101057.
[11] K.-T. Yong, H. Ding, I. Roy, W.-C. Law, E.J. Bergey, A. Maitra, P.N. Prasad, Imaging Pancreatic Cancer Using Bioconjugated InP Quantum Dots, ACS Nano. 3 (2009) 502–510, https://doi.org/10.1021/nn8008933.
[12] R. Xie, M. Rutherford, X. Peng, Formation of High-Quality I–III–VI Semiconductor Nanocrystals by Tuning Relative Reactivity of Cationic Precursors, J. Am. Chem. Soc. 131 (2009) 5691–5697, https://doi.org/10.1021/ja9005767.
[13] J. Hofhuis, J. Schoonman, A. Goossens, Elucidation of the Excited-State Dynamics in CuInS2 Thin Films, J. Phys. Chem. C. 112 (2008) 15052–15059, https://doi.org/10.1021/jp803307e.
[14] P.-H. Chuang, C. Che Lin, R.-S. Liu, Emission-Tunable CuInS2/ZnS Quantum Dots: Structure, Optical Properties, and Application in White Light-Emitting Diodes with High Color Rendering Index, ACS Appl. Mater. & Interfaces. 6 (2014) 15379–15387, https://doi.org/10.1021/am503889z.
[15] W.-S. Song, H. Yang, Efficient White-Light-Emitting Diodes Fabricated from Highly Fluorescent Copper Indium Sulfide Core/Shell Quantum Dots, Chem. Mater. 24 (2012) 1961–1967, https://doi.org/10.1021/cm300837z.
[16] R. Jose Varghese, S. Parani, V.R. Remya, R. Maluleke, S. Thomas, O.S. Oluwafemi, Sodium alginate passivated CuInS2/ZnS QDs encapsulated in the mesoporous channels of amine modified SBA 15 with excellent photostability and biocompatibility, Int. J. Biol. Macromol. 161 (2020) 1470–1476, https://doi.org/10.1016/J.IJBIOMAC.2020.07.240.
[17] H. Zhong, Y. Zhou, M. Ye, Y. He, J. Ye, C. He, C. Yang, Y. Li, Controlled Synthesis and Optical Properties of Colloidal Ternary Chalcogenide CuInS2 Nanocrystals, Chem. Mater. 20 (2008) 6434–6443, https://doi.org/10.1021/cm8006827.

[18] L. Li, T. Jean Daou, I. Texier, T. Thi Kim Chi, N. Quang Liem, P. Reiss, Highly Luminescent CuInS2/ZnS Core/Shell Nanocrystals: Cadmium-Free Quantum Dots for In Vivo Imaging, Chem. Mater. 21 (2009) 2422–2429. https://doi.org/10.1021/cm900103b.
[19] P.M. Allen, M.G. Bawendi, Ternary I−III−VI Quantum Dots Luminescent in the Red to Near-Infrared, J. Am. Chem. Soc. 130 (2008) 9240–9241, https://doi.org/10.1021/ja8036349.
[20] H. Zhong, Z. Wang, E. Bovero, Z. Lu, F.C.J.M. van Veggel, G.D. Scholes, Colloidal CuInSe2 Nanocrystals in the Quantum Confinement Regime: Synthesis, Optical Properties, and Electroluminescence, J. Phys. Chem. C. 115 (2011) 12396–12402, https://doi.org/10.1021/jp204249j.
[21] B. Mao, C.-H. Chuang, J. Wang, C. Burda, Synthesis and Photophysical Properties of Ternary I-III–VI AgInS2 Nanocrystals: Intrinsic versus Surface States, J. Phys. Chem. C. 115 (2011) 8945–8954, https://doi.org/10.1021/jp2011183.
[22] T. Uematsu, T. Doi, T. Torimoto, S. Kuwabata, Preparation of Luminescent AgInS2−AgGaS2 Solid Solution Nanoparticles and Their Optical Properties, J. Phys. Chem. Lett. 1 (2010) 3283–3287, https://doi.org/10.1021/jz101295w.
[23] J. Krustok, J. Raudoja, J.H. Schön, M. Yakushev, H. Collan, The role of deep donor–deep acceptor complexes in CIS-related compounds, Thin Solid Films. 361–362 (2000) 406–410, https://doi.org/10.1016/S0040-6090(99)00756-7.
[24] S.T. Ahamed, C. Kulsi, D. Kirti, D.N. Banerjee, A.M. Srivastava, Synthesis of multifunctional CdSe and Pd quantum dot decorated CdSe thin films for photocatalytic, electrocatalytic and thermoelectric applications, Surfaces and Interfaces. 25 (2021), 101149, https://doi.org/10.1016/J.SURFIN.2021.101149.
[25] R. Koole, P. Liljeroth, S. Oosterhout, D. Vanmaekelbergh, Chemisorption Determines the Photovoltage of a Ti/TiO2/Au/Dye Internal Electron Emission Photovoltaic Cell, J. Phys. Chem. B. 109 (2005) 9205–9208, https://doi.org/10.1021/jp051344k.
[26] C.W. Lee, C.H. Chou, J.H. Huang, C.S. Hsu, T.P. Nguyen, Investigations of organic light emitting diodes with CdSe(ZnS) quantum dots, Mater. Sci. Eng. B. 147 (2008) 307–311, https://doi.org/10.1016/J.MSEB.2007.09.068.
[27] Y.-Q. Li, Y. Yang, C.Q. Sun, S.-Y. Fu, Significant Enhancements in the Fluorescence and Phosphorescence of ZnO Quantum Dots/SiO2 Nanocomposites by Calcination, J. Phys. Chem. C. 112 (2008) 17397–17401, https://doi.org/10.1021/jp8063068.
[28] K.S. Leschkies, R. Divakar, J. Basu, E. Enache-Pommer, J.E. Boercker, C. Barry Carter, U.R. Kortshagen, D.J. Norris, E.S. Aydil, Photosensitization of ZnO Nanowires with CdSe Quantum Dots for Photovoltaic Devices, Nano Lett. 7 (2007) 1793–1798, https://doi.org/10.1021/nl070430o.
[29] W. Sheng, S. Kim, J. Lee, S.-W. Kim, K. Jensen, M.G. Bawendi, In-Situ Encapsulation of Quantum Dots into Polymer Microspheres, Langmuir. 22 (2006) 3782–3790, https://doi.org/10.1021/la0519731.
[30] J. Lee, V.C. Sundar, J.R. Heine, M.G. Bawendi, K.F. Jensen, Full Color Emission from II ± VI Semiconductor, Adv. Mater. 12 (2000) 1102–1105.
[31] P. Govindaraj, A. Sokolova, N. Salim, S. Juodkazis, F.K. Fuss, B. Fox, N. Hameed, Distribution states of graphene in polymer nanocomposites: A review, Compos. Part B Eng. 226 (2021), 109353, https://doi.org/10.1016/J.COMPOSITESB.2021.109353.
[32] W.J.E. Beek, M.M. Wienk, R.A.J. Janssen, Hybrid solar cells from regioregular polythiophene and ZnO nanoparticles, Adv. Funct. Mater. 16 (2006) 1112–1116, https://doi.org/10.1002/adfm.200500573.
[33] S. Mohan, O.S. Oluwafemi, S.P. Songca, O.A. Osibote, S.C. George, N. Kalarikkal, S. Thomas, Facile synthesis of transparent and fluorescent epoxy-CdSe-CdS-ZnS core-multi shell polymer nanocomposites, New J. Chem. 38 (2014) 155–162, https://doi.org/10.1039/c3nj00659j.
[34] M. Wang, L. Ma, L. Shi, P. Feng, X. Wang, Y. Zhu, G. Wu, G. Song, Chemical grafting of nano-SiO2 onto graphene oxide via thiol-ene click chemistry and its effect on the interfacial and mechanical properties of GO/epoxy composites, Compos. Sci. Technol. 182 (2019), 107751, https://doi.org/10.1016/j.compscitech.2019.107751.
[35] N. Ning, M. Wang, G. Zhou, Y. Qiu, Y. Wei, Effect of polymer nanoparticle morphology on fracture toughness enhancement of carbon fiber reinforced epoxy composites, Compos. Part B Eng. 234 (2022), 109749, https://doi.org/10.1016/J.COMPOSITESB.2022.109749.
[36] S.K. Shin, H.J. Yoon, Y.J. Jung, J.W. Park, Nanoscale controlled self-assembled monolayers and quantum dots, Curr. Opin. Chem. Biol. 10 (2006) 423–429, https://doi.org/10.1016/J.CBPA.2006.08.006.
[37] S.V. Kershaw, A.L. Rogach, Infrared emitting HgTe quantum dots and their waveguide and optoelectronic devices, Zeitschrift Fur Phys, Chemie. 229 (2015) 23–64, https://doi.org/10.1515/zpch-2014-0590.
[38] M.A. Uddin, H.P. Chan, Materials and process optimization in the reliable fabrication of polymer photonic devices, J. Optoelectron. Adv. Mater. 10 (2008) 1–17.
[39] H. Wang, K.S. Lee, J.H. Ryu, C.H. Hong, Y.H. Cho, White light emitting diodes realized by using an active packaging method with CdSe/ZnS quantum dots dispersed in photosensitive epoxy resins, Nanotechnology. 19 (2008), https://doi.org/10.1088/0957-4484/19/14/145202.
[40] W. Zou, Z.J. Du, H.Q. Li, C. Zhang, A transparent and luminescent epoxy nanocomposite containing CdSe QDs with amido group-functionalized ligands, J. Mater. Chem. 21 (2011) 13276–13282, https://doi.org/10.1039/c1jm11125f.
[41] Z. Zhao, S. Yin, W. Luan, S.T. Tu, Metal Structural Integrity Monitoring via Optical Response of Quantum Dots-epoxy Resin, Energy Procedia. 75 (2015) 2061–2067, https://doi.org/10.1016/J.EGYPRO.2015.07.291.
[42] S. Wang, As featured in, 2011. https://doi.org/10.1039/c1jm00061f.
[43] Y. Yang, Y.-Q. Li, S.-Y. Fu, H.-M. Xiao, Transparent and Light-Emitting Epoxy Nanocomposites Containing ZnO Quantum Dots as Encapsulating Materials for Solid State Lighting, J. Phys. Chem. C. 112 (2008) 10553–10558, https://doi.org/10.1021/jp802111q.
[44] B. Chen, H. Zhong, W. Zhang, Z. Tan, Y. Li, C. Yu, T. Zhai, Y. Bando, S. Yang, B. Zou, Highly emissive and color-tunable CuInS 2-based colloidal semiconductor nanocrystals: Off-stoichiometry effects and improved electroluminescence performance, Adv. Funct. Mater. 22 (2012) 2081–2088, https://doi.org/10.1002/adfm.201102496.
[45] C.B. Murray, D.J. Norris, M.G. Bawendi, Synthesis and characterization of nearly monodisperse CdE (E = sulfur, selenium, tellurium) semiconductor nanocrystallites, J. Am. Chem. Soc. 115 (2002) 8706–8715, https://doi.org/10.1021/ja00072a025.
[46] H. Nakamura, W. Kato, M. Uehara, K. Nose, T. Omata, S. Otsuka-Yao-Matsuo, M. Miyazaki, H. Maeda, Tunable Photoluminescence Wavelength of Chalcopyrite CuInS2-Based Semiconductor Nanocrystals Synthesized in a Colloidal System, Chem. Mater. 18 (2006) 3330–3335, https://doi.org/10.1021/cm0518022.